Artificial Muscles from Fishing Line and Sewing Thread

Carter S. Haines *et al.*

Science **343**, 868 (2014);
DOI: 10.1126/science.1246906

Artificial Muscles from Fishing Line and Sewing Thread

Carter S. Haines,[1] Márcio D. Lima,[1] Na Li,[1] Geoffrey M. Spinks,[2] Javad Foroughi,[2] John D. W. Madden,[3] Shi Hyeong Kim,[4] Shaoli Fang,[1] Mônica Jung de Andrade,[1] Fatma Göktepe,[5] Özer Göktepe,[5] Seyed M. Mirvakili,[3] Sina Naficy,[2] Xavier Lepró,[1] Jiyoung Oh,[1] Mikhail E. Kozlov,[1] Seon Jeong Kim,[4] Xiuru Xu,[1,6] Benjamin J. Swedlove,[1] Gordon G. Wallace,[2] Ray H. Baughman[1]*

The high cost of powerful, large-stroke, high-stress artificial muscles has combined with performance limitations such as low cycle life, hysteresis, and low efficiency to restrict applications. We demonstrated that inexpensive high-strength polymer fibers used for fishing line and sewing thread can be easily transformed by twist insertion to provide fast, scalable, nonhysteretic, long-life tensile and torsional muscles. Extreme twisting produces coiled muscles that can contract by 49%, lift loads over 100 times heavier than can human muscle of the same length and weight, and generate 5.3 kilowatts of mechanical work per kilogram of muscle weight, similar to that produced by a jet engine. Woven textiles that change porosity in response to temperature and actuating window shutters that could help conserve energy were also demonstrated. Large-stroke tensile actuation was theoretically and experimentally shown to result from torsional actuation.

Artificial muscle fibers are needed for diverse applications, ranging from humanoid robots, prosthetic limbs, and exoskeletons to comfort-adjusting clothing and miniature actuators for microfluidic "laboratories on a chip." However, performance, scalability, and cost problems have restricted their deployment. Electrothermally driven shape-memory metal wires can contract fast and deliver large strokes under heavy loads, but are expensive and hysteretic, which makes them difficult to control (*1*, *2*). Thermally powered shape-memory polymers have low work capacity unless they are fiber-reinforced (*3, 4*), and giant-work-capacity polymer/carbon nanotube (CNT) composite fibers must be redrawn between cycles (*5*). High-performance hybrid CNT muscles (*6*), in which a guest (such as paraffin wax) is infiltrated into a twist-spun carbon nanotube yarn, are expensive because of the cost of CNT yarn. Electrochemically driven fibers of organic conducting polymers can provide large strokes but have limited cyclability and cycle rate and require an electrolyte, counter-electrode, and containment system, which adds to system weight and cost (*7*–*9*). Polymeric electric field–driven electrostrictive rubbers and relaxor ferroelectrics (*10*–*12*) are attractive because of their large strokes and high efficiencies but would be difficult to deploy as muscle-like fibers because of the high required electric fields.

The present goal is to convert inexpensive (~$5/kg) high-strength polymer fibers into artificial muscles that match or exceed the performance of mammalian skeletal muscle to deliver millions of reversible contractions and over 20% tensile stroke, while rapidly lifting heavy loads. These muscles should provide hysteresis-free actuation to enable convenient control, be scalable in force-lifting capability without decreasing stroke or gravimetric work capabilities, and be weavable into textiles that actuate to accomplish amplified mechanical work or change textile porosity.

We started from low-cost high-strength fibers, most often those used as fishing line or sewing thread (table S1). Commercially produced polyethylene and nylon fibers are important muscle precursors, because they combine reversible–fiber-direction thermal contraction, large volumetric thermal expansion, and large anisotropy in thermally induced dimension changes to provide enhanced muscle stroke.

These precursor fibers are composed of flexible polymer chains that are highly oriented in the fiber direction. Although crystalline regions of highly drawn polymers, such as polyethylene and nylon, can have small negative thermal expansion coefficients (*13*), fiber-direction–aligned polymer chains in neighboring noncrystalline regions are less conformationally constrained, so they can provide large reversible contractions as they access conformational entropy when heated (*14*, *15*) (fig. S1). The resulting thermal contraction of nylon 6,6 fibers (Fig. 1A) can be as large as 4% (Fig. 2A and fig. S2A), which is similar to that of commercial NiTi shape-memory wires.

As with CNT yarn muscles (*6*, *16*), twist is inserted into these polymer fibers to make them

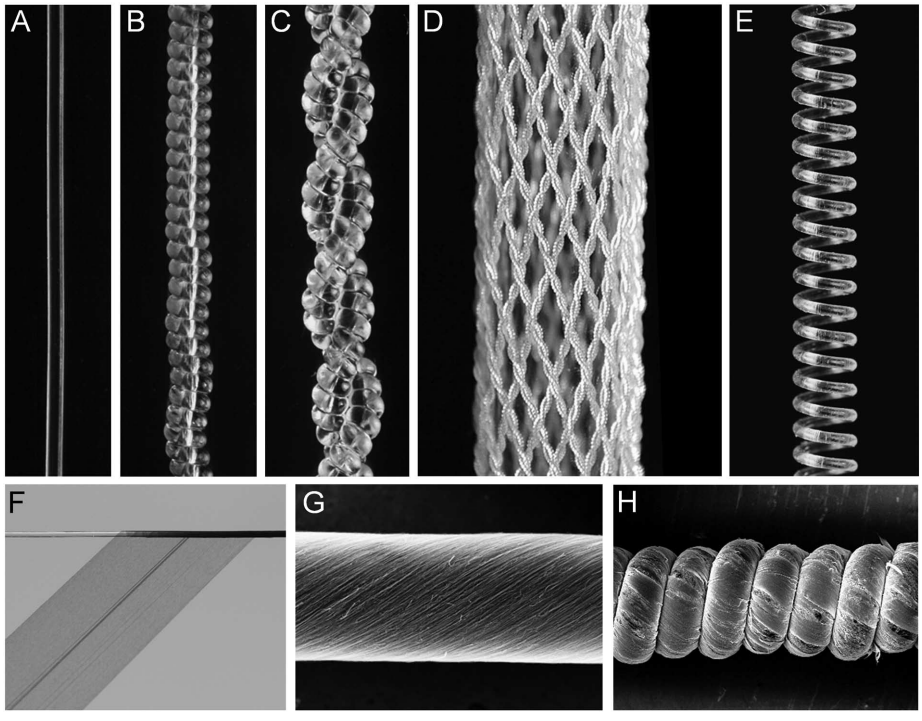

Fig. 1. Muscle and precursor structures using nylon 6,6 monofilament sewing thread. Optical images of (**A**) a nontwisted 300-μm-diameter fiber; (**B**) the fiber of (A) after coiling by twist insertion; (**C**) a two-ply muscle formed from the coil in (B); (**D**) a braid formed from 32 two-ply, coiled, 102-μm-diameter fibers produced as in (C); (**E**) a 1.55-mm-diameter coil formed by inserting twist in the fiber of (A), coiling it around a mandrel, and then thermally annealing the structure; and (**F**) helically wrapping the fiber of (A) with a forest-drawn CNT sheet and scanning electron microscope images of a CNT-wrapped, 76-μm-diameter nylon 6,6 monofilament (**G**) before and (**H**) after coiling by twist insertion.

[1]The Alan G. MacDiarmid NanoTech Institute, University of Texas at Dallas, Richardson, TX 75083, USA. [2]Intelligent Polymer Research Institute, ARC Centre of Excellence for Electromaterials Science, University of Wollongong, Wollongong, New South Wales 2522, Australia. [3]Department of Electrical and Computer Engineering and Advanced Material and Process Engineering Laboratory, University of British Columbia, Vancouver, British Columbia V6T 1Z4, Canada. [4]Center for Bio-Artificial Muscle and Department of Biomedical Engineering, Hanyang University, Seoul 133-791, South Korea. [5]Department of Textile Engineering, Çorlu Engineering Faculty, Namık Kemal University, Çorlu-Tekirdağ, Turkey. [6]Alan G. MacDiarmid Institute, Jilin University, Changchun 130012, China.

*Corresponding author. E-mail: ray.baughman@utdallas.edu

chiral, which enables them to function as torsional muscles. Most importantly, we greatly amplified tensile stroke by inserting such a large amount of twist that some twist converted to fiber coiling (movie S1), called writhe (*17*, *18*). By completely coiling the fibers (Fig. 1B), tensile contractions (Fig. 2A) exceeding the maximum in vivo stroke of human skeletal muscles (~20%) (*19*) were obtained. This coiling is more compact than that used to amplify the stroke of shape-memory metal wires, thereby providing contraction against higher applied stress (19 MPa for nylon) than reported for NiTi coils (~1.6 MPa) (*1*), in which stress is obtained by normalization to the nonactuated coil's cross-sectional area. The spring index (*C*), the ratio of mean coil diameter to the fiber diameter, for such polymer muscles will typically be less than 1.7, whereas for NiTi coils this ratio exceeds 3.0.

The weight applied during coiling is important and is adjustable over a narrow range for a given fiber: Too little weight and the fiber snarls during twist insertion; too much weight and the fiber breaks. For example, the load during coiling can be varied between 10 and 35 MPa for a 127-μm-diameter nylon 6,6 sewing thread, yielding coils with spring indices between 1.7 and 1.1, respectively. Immediately after coiling, adjacent coils are in contact, limiting contraction during actuation, and must be separated by increasing load or reducing twist.

Coils formed by twist insertion maintain some twist liveliness, meaning that they can untwist, especially when under load. This problem can be avoided by preventing end rotation during actuation, by thermal annealing to set the structure, or by forming torque-balanced structures. Figure 1C depicts a coiled polymer muscle that has been torque-balanced by plying (in the *Z* direction) two S-twisted fibers. Thereby stabilized, the plied, highly coiled muscles can be woven into textiles or braids (Fig. 1D).

Coiled muscles can also be made by wrapping highly twisted fibers around a mandrel and then stabilizing the coils by thermal annealing (Fig. 1E). This process enables the formation of larger-diameter coils than by direct, unconfined (i.e., mandrel-free) twist insertion. Although such structures have reduced load capacity, they can contract more before adjacent coils contact, thereby achieving larger stroke. The relative directions and amounts of twist in the fibers and the coils can be varied using this method. When the chirality of fiber twist matches the coil's chirality, the muscle contracts during heating. However, when these chiralities are opposite, the coiled polymer muscle expands during heating (movie S2). We hereafter refer to such coils as homochiral and heterochiral, respectively.

Thermomechanical analysis (TMA) results for fiber thermal expansion before and after coiling are shown in Fig. 2A for four polymer fibers (Table 1 and table S1). Unless otherwise indicated, tensile stress and modulus are calculated as nominal values by normalizing applied force to the diameter of the initial nontwisted fiber, because coil and fiber diameter are difficult to measure accurately during isotonic (constant applied force) measurements, where coil diameter varies during large-stroke actuation. Gravimetric capabilities were used to provide performance comparisons between natural and artificial muscles.

The reversible thermal contraction of nylon 6,6 monofilament between 20° and 240°C increased from 4 to 34% as a result of coiling (Fig. 2A and fig. S2). Polyethylene's lower melting temperature limited contraction to less than 0.3% for the noncoiled fiber and 16% for the coiled muscle between 20° and 130°C. However, the higher modulus and strength of coiled polyethylene

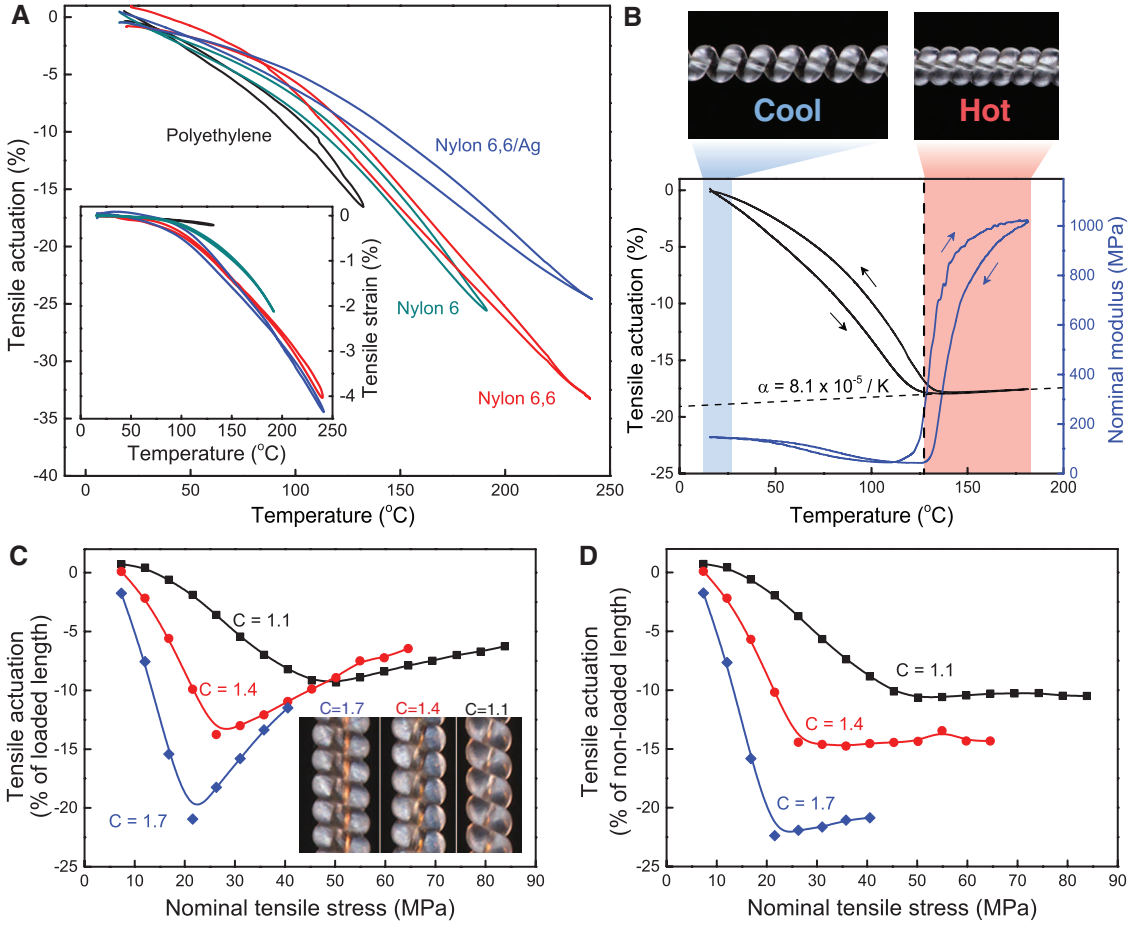

Fig. 2. Thermomechanical analysis of various muscles. (**A**) Comparison of the negative thermal expansion of braided polyethylene, nylon 6 monofilament, nylon 6,6 monofilament, and silver-coated nylon 6,6 multifilament fibers before twisting (inset) and after coiling by twist insertion. (**B**) Tensile stroke and nominal modulus versus temperature for a coiled, 300-μm-diameter nylon 6,6 monofilament muscle under 7.5 MPa static and 0.5 MPa dynamic load. During contraction, neighboring coils come into complete contact at ~130°C, which dramatically increases nominal elastic modulus and causes the thermal expansion coefficient to become positive. Optical micrographs (top) are shown of the coils before and after contact. (**C**) Tensile stroke versus load, as a percent of the loaded muscle length, for a 127-μm-diameter nylon 6,6 monofilament fiber that was coiled by twist insertion under loads of 10, 16, and 35 MPa, which resulted in spring indices of 1.7, 1.4, and 1.1, respectively. Optical images of the coils are inset. (**D**) The results of (C) when normalized to the initial nonloaded muscle length, indicating that the absolute displacement during actuation remains nearly constant at loads above those at which coils contact.

fibers (a nearly 10 times higher nominal modulus than for coiled nylon, fig. S8) are especially useful for muscles that lift heavy loads and provide increased energy efficiency.

When adjacent coils contact, due to insufficient applied load or excessive twist, the muscle-direction thermal expansion becomes positive, as in Fig. 2B. Under low tensile load (7.5 MPa), upon coil contact at ~130°C, the nylon 6,6 muscle expands at a rate comparable to the fiber's radial thermal expansion. After inter-coil contact, the coiled structure stiffens with increasing temperature, producing a 24-fold increase in nominal tensile modulus (Fig. 2B). Such large temperature-controlled changes in compliance may be useful for humanoid robots, in which actions such as catching a ball require both tensile actuation and tunable stiffness.

The tensile stroke and load-carrying capabilities of coiled muscles can be varied by adjusting the coil spring index, which is inversely related to spring stiffness (*1*). Figure 2C plots the load dependence of tensile stroke for coils having spring indices of 1.1, 1.4, and 1.7, produced by coiling under stresses of 10, 16, and 35 MPa, respectively. For each muscle, maximum stroke was realized for the lowest applied load (called the optimal load) that prevented inter-coil contact over the temperature range used (20° to 120°C). For the largest diameter coil (C = 1.7), this maximum stroke (21%) occurred for an optimal load of 22 MPa. When the polymer muscle was tightly coiled (C = 1.1), the maximum stroke decreased to 9.3%, but the optimal load increased to 50 MPa. Large-diameter mandrel-formed coils can yield even larger strokes, such as the 49% contraction provided at 1 MPa for a nylon 6 fiber having C = 5.5 (movie S2).

When coils are noncontacting, absolute stroke and stroke normalized to the nonloaded muscle length do not substantially depend on applied load (Fig. 2D), even though stroke normalized to loaded initial muscle length decreases with increasing load (Fig. 2C) because of muscle lengthening. Hence, the work done during contraction increases up to loads where the muscle breaks. The maximum specific work during contraction was 2.48 kJ/kg for the C = 1.1 nylon 6,6 muscle of Fig. 2C (*1*), which is 64 times that for natural muscle (*19*). The average mechanical output power during contraction (27.1 kW/kg) was 84 times the peak output of mammalian skeletal muscles (0.323 kW/kg) (*1*, *20*). However, although natural muscles have a typical energy conversion efficiency of 20%, the maximum energy conversion efficiency during contraction was 1.08 and 1.32% for the coiled nylon and polyethylene fibers, respectively (*1*). These polymer muscle efficiencies are similar to those of commercial shape-memory metals, which can reach 1 or 2% (*21*).

Shape-memory NiTi muscles suffer from over 20°C hysteresis in stroke, complicating actuator control (*2*, *22*). Scanning at a slow 2°C/min rate, to reduce artificial hysteresis due to temperature measurement errors, reveals that coiled nylon 6,6 actuators exhibit little or no inherent hysteresis (less than 1.2°C, Fig. 3A). This substantial absence of hysteresis, combined with the far more linear temperature dependence than for the commercially important NiTi shape-memory wires, makes these coiled polymer fiber muscles well suited for robotics and prosthetics, where a continuous range of control is desired. Although very recent work has provided shape-memory metal wires exhibiting down to 2°C hysteresis, these muscles comprise ~56.5 weight % gold (*23*).

Although such muscles can be driven chemically, photonically, hydrothermally, or by ambient temperature changes (*1*), electrothermally driven muscles must contain an electrical heating element. This can be provided by helically wrapping the coiled muscle or precursor fiber with a CNT sheet (*24*) (Fig. 1F-1H), using commercial metal-coated sewing thread, or placing a conductor on the inside or outside of the coiled muscle fiber (such as wires woven into an actuating textile or placed interior to actuating fiber braids, movies S5 and S6).

A coiled nylon 6,6 muscle delivered over 1 million cycles during periodic actuation at 1 Hz (Fig. 3B), raising and lowering a 10-g weight producing 22 MPa of nominal stress. This actuation was powered by applying a 30 V/cm square-wave potential (normalized to coil length) at a 20% duty cycle. Although the coiled fiber did experience creep (inset of Fig. 3B), this creep was below 2% over the 1.2 million investigated cycles, stroke amplitude was negligibly affected, and the creep rate decreased with cycling.

Similar to other thermally or electrochemically driven artificial muscles, muscle cycle rate decreases with increasing fiber diameter. This response time is unimportant when harvesting energy from slowly varying ambient temperature changes or for clothing textiles that change porosity to provide wearer comfort, but it is critically important when maximizing average output power. Passive cooling offers an economical solution to increase cycle rate. For instance, when immersed in water, a two-ply, coiled, silver-plated, 180-μm-diameter nylon fiber can be electrothermally actuated at 5 Hz to produce ~10% stroke while lifting a 22-MPa load (movie S4). Similarly, in helium, a coiled, 26-μm-diameter CNT-wrapped, nylon 6,6 monofilament was capable of actuation at over 7.5 Hz (*1*).

Fast, high-force actuation can be driven hydrothermally. A coiled polymer muscle made from 860-μm-diameter nylon 6 fishing line (Fig. 4, A and B) was driven at 1 Hz by switching between cold (~25°C) and hot (95°C) water (movie S3), achieving 12% reversible actuation under a 0.5-kg load (8.4 MPa). Even though nylon muscles absorb water (*25*), 1500 reversible actuation cycles were observed.

Polyethylene fiber muscles, which do not absorb water, can similarly be driven hydrothermally if a surfactant (dishwashing soap) is added to facilitate polymer wetting. A coiled polyethylene muscle was prepared by twisting an 800-μm-diameter bundle of four polyethylene fishing lines. Containing the muscle in a flexible silicone tube to allow fast water flow provided 4.5% contraction at 2 Hz while lifting a 7.2 kg (140 MPa) load (movie S3). The mechanical work output during contraction (2.63 kJ/kg), normalized to the total cycle time, was 5.26 kW/kg (7.1 horsepower/kg), which is over 100 times that of a human biceps muscle (*26*) and roughly the same as for a modern jet engine (*27*).

Polymer fibers that are twisted, but not coiled, are capable of producing surprisingly large amounts of mechanical work as torsional actuators. Constant-torque torsional actuation measurements were performed (using the apparatus of fig. S5) on an 860-μm-diameter, 5.5-cm-long, twisted nylon 6 fiber. When heated from 20° to 160°C, this muscle lifted a 1-kg load by 7 mm by rotating a 2.8-mm-diameter axle by 286°, thereby providing 2.1 kJ/kg of mechanical work (Fig. 3D). This work during rotation is similar to the 2.48 kJ/kg provided during tensile actuation of a coiled nylon 6,6 muscle.

Why do two-end–tethered, fully coiled homochiral polymer fibers thermally contract during heating, independent of whether the nontwisted fibers have a positive or negative axial thermal expansion coefficient (fig. S2), and why is such thermal contraction so large? The answers are found in the ability of twisted fibers to generate giant torque by reversibly untwisting when heated, as shown in Fig. 3C.

Until just before coiling, initially parallel polymer chains are twisted into helices that have a bias angle relative to the fiber direction of approximately

$$\alpha_f = \tan^{-1}(2\pi rT) \qquad (1)$$

where r is the radial distance from the fiber center and T is the amount of twist inserted per initial fiber length.

Table 1. Summary of the polymer fibers found to be most useful for actuation as coiled tensile muscles, and the parameters used to fully coil them. The tensile actuation results are given in Fig. 2A.

Material	Diameter (μm)	Load during coiling (MPa)	Twist to coil (turns/m)
Nylon 6 monofilament fishing line	270	17	1430
Nylon 6,6 monofilament sewing thread	127	16	3020
Nylon 6,6 silver-plated multifilament sewing thread	180	14	2430
Polyethylene braided fishing line	130	37	2270

After twisting, both length contraction of these helically configured polymer chains and fiber diameter expansion will cause fiber untwist (*1*). To enable physical understanding, consider the case where these effects are artificially decoupled, so that polymer chain length contracts while the fiber diameter is kept constant, or fiber diameter increases while the polymer chain length is kept constant. Both cases result in fiber untwist. Although thermal untwist can occur in any fiber whose radial expansion exceeds its axial expansion, polymers such as nylon are ideal because negative

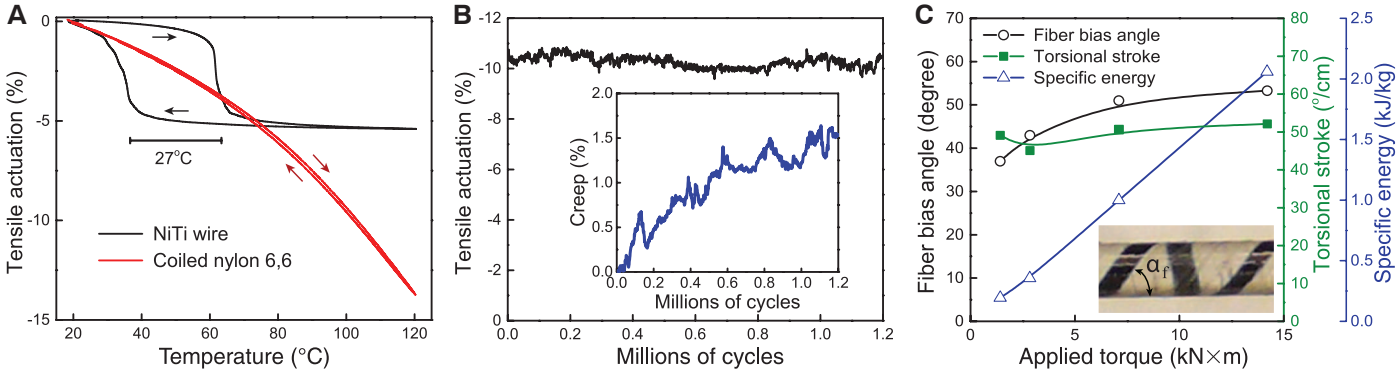

Fig. 3. Performance of torsional and tensile artificial muscles. (**A**) Comparison of hysteresis for a 152-μm-diameter NiTi wire muscle and a coiled, 127-μm-diameter nylon 6,6 monofilament muscle, measured using a 2°C/min scan rate. Less than 1.2°C of hysteresis is observed for the nylon muscle versus the 27°C hysteresis for the NiTi muscle. (**B**) Tensile actuation versus cycle for a coiled, 76-μm-diameter, nylon 6,6 monofilament wrapped in a CNT sheet and driven electrothermally at 1 Hz under a 22-MPa load (each point averages 1000 cycles). The inset provides creep as a function of cycle. (**C**) The optically measured fiber bias angle induced by an applied torque and the torsional stroke and work during thermal actuation (between 20° and 160°C) as a function of this applied torque for a noncoiled torsional muscle made from 860-μm-diameter nylon 6 fishing line (*1*). The inset photograph was used to optically determine the fiber bias angle by measuring the displacement of a black line from its initial orientation parallel to the fiber axis.

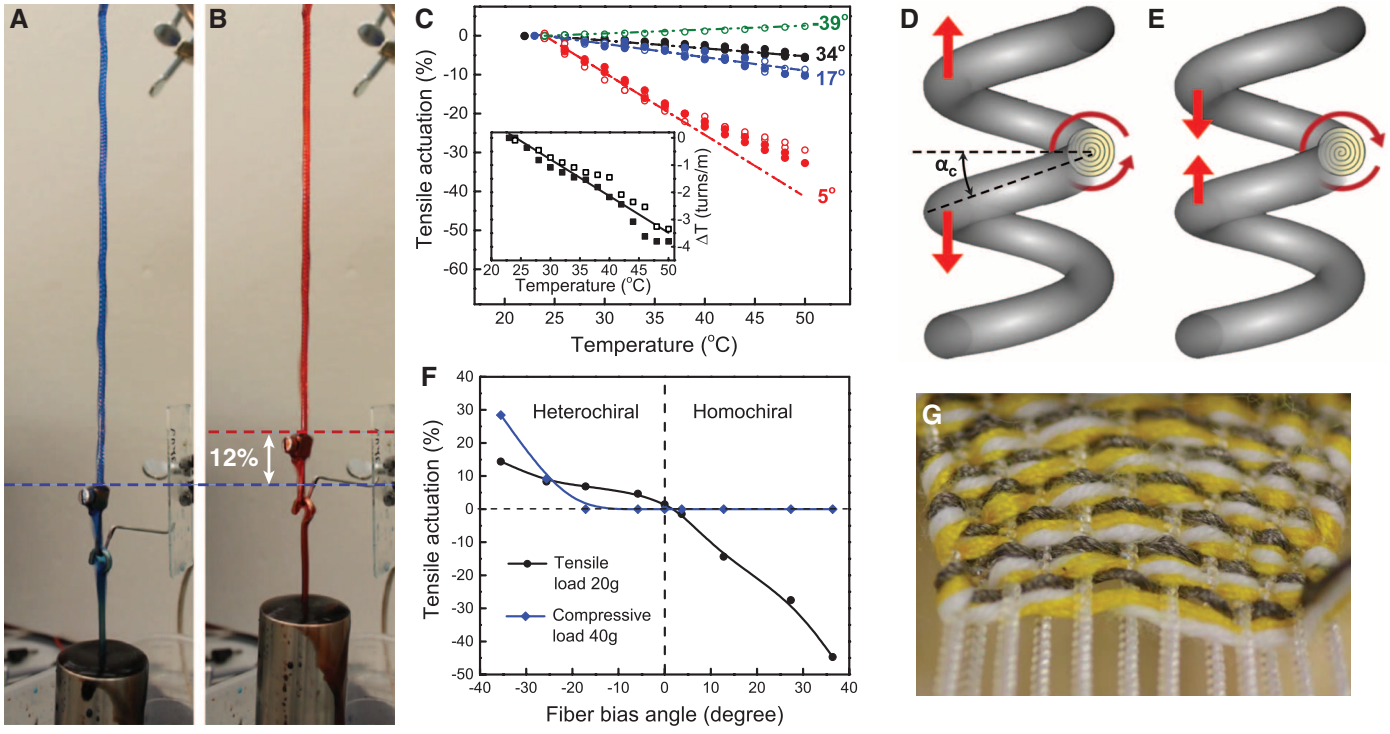

Fig. 4. Mechanism and applications for coiled polymer muscles. Hydrothermal actuation of a coiled 860-μm-diameter nylon 6 fishing line lifting a 500-g load by 12% when switched at 0.2 Hz between (**A**) ~25°C water (dyed blue) and (**B**) 95°C water (dyed red). (**C**) Calculated temperature dependence of tensile actuation (dashed lines) compared to experimental results (using an applied stress of 2.2 MPa, solid symbols, and 3.1 MPa, open symbols, respectively) for twisted 450-μm-diameter, nylon 6 monofilament fibers that are mandrel-wrapped to the indicated initial coil bias angles (*1*). Contracting and expanding coils were homochiral and heterochiral, respectively. From Eq. 3, fiber untwist during heating was calculated for the coiled fiber with a 17° bias angle to provide the data in the inset, which was then used to predict tensile actuation for the other coiled fibers. (**D** and **E**) Schematic illustration of the mechanism by which torsional fiber actuation drives large-stroke tensile actuation for (D) heterochiral and (E) homochiral coiled fibers. (**F**) Measured tensile actuation versus fiber bias angle for coiled, 860-μm-diameter nylon 6 muscles actuated between 25° and 95°C. These results show, for highly twisted fibers, that the homochiral muscles thermally contract when coils are noncontacting, and the heterochiral muscles expand. (**G**) An actuating textile woven from conventional polyester, cotton, and silver-plated nylon (to drive electrothermal actuation) yarn in the weft direction and coiled nylon monofilament muscle fibers in the warp direction.

axial expansion and positive radial expansion additively contribute to untwist.

This thermally induced fiber untwist (ΔT, measured in turns per initial fiber length) generates the torsional actuation observed for twisted fibers and drives the length change for coiled fibers by requiring coil bias angle to change from α_c to α_c', as described by the spring mechanics equation (*28*)

$$\Delta T = \frac{\sin(\alpha_c')\cos(\alpha_c')}{\pi D'} - \frac{\sin(\alpha_c)\cos(\alpha_c)}{\pi D} \quad (2)$$

where D and D' are the coil diameters, taken through the fiber centerline before and after heating, and the coil bias angle α_c is the angle between the fiber and the coil's cross-section. For a coil of N turns and length L made from a fiber of length l: $\sin(\alpha_c) = L/l$ and $\cos(\alpha_c) = \pi ND/l$. Using these relationships and assuming negligible change in fiber length l (fig. S4), stretching a coil clamped to prevent end rotation creates a change in fiber twist of

$$\Delta T = \frac{N\Delta L}{l^2} \quad (3)$$

From this equation, we can predict the giant contractions and expansions in coil length resulting from fiber untwist during heating [Fig. 4C and table S2 (*1*)]. This twist-driven coil actuation mechanism is best demonstrated using mandrel-formed coils. Upon heating of a homochiral muscle, the fiber generates an untwisting torque that pulls coils together, providing work by contracting in length (Fig. 4E). Conversely, when oppositely twisted and coiled to form a heterochiral muscle, fiber untwist during heating increases coil length (Fig. 4D). This relationship is depicted in Fig. 4F, which shows, for highly twisted fibers, that the strokes for homochiral and heterochiral coils are maximized when using tensile and compressive loads, respectively. For compressive loads, the homochiral muscle stroke is near zero because adjacent coils are in contact. By preventing inter-coil contact, thermally driven fiber untwist can cause giant muscle contraction (>45%, Fig. 4F and movie S2).

Retention of muscle stroke and specific work capacity as fiber diameter changes by orders of magnitude is important for the diverse family of targeted applications, ranging from microscopic actuators for microfluidic circuits to those for giant-force-capacity exoskeletons and morphing air vehicles. Present experimental results for twist-insertion–coiled nylon 6 (150- to 2.45-mm-diameter fibers coiled under 16 MPa of nominal stress) provided nearly constant percent stroke and specific energy during contraction against 32 MPa of nominal stress (fig. S9, *1*), despite spanning a 267-fold range in cross-sectional area and a 325-fold range in load rating for precursor fishing lines (0.91 to 295 kg).

This near-invariance of actuator performance with fiber diameter implies near-perfect scaling of structure and therefore of properties. Indeed, we find to good approximation that the twist insertion per muscle length needed to initiate and complete coiling is inversely proportional to precursor fiber diameter (fig. S10B). This means that the fiber bias angle is nearly scale-invariant, and the number of coils per fiber length inversely depends on fiber diameter. Hence, images of twist-insertion–coiled fibers having vastly different diameters look much the same when scaled by adjusting magnification to have the same diameter (fig. S10A).

The performance of coiled muscle fibers suggests many possible applications, such as for window shutters that noiselessly open and close to conserve energy (movie S8). Additionally, spools of both conductive and nonconductive nylon are cheaply obtainable, used in clothing, and easily processed into high-stroke artificial muscles. These advantages encourage incorporating coiled fiber muscles in actuating textiles and braids.

Figure 1D shows a braid produced from 32 two-ply coils of 102-μm-diameter nylon fiber. This braid was used as a sleeve over a glass tube containing a nichrome heating element. Upon heating to 120°C, the braid delivered 16.4% stroke while lifting a 630-g load (movie S6). During contraction, the structure of the braid changed (fig. S10), decreasing the braid helix angle from 66.2° to 62.1°, corresponding to a 20.6% drop in pore area. Figure 4G shows a textile woven from coiled nylon muscles, conductive silver-plated fibers for electrothermal heating, and polyester and cotton fibers. Twelve muscle fibers were deployed in parallel to lift 3 kg (movie S5), while providing increased cycle rate capabilities by dissipating heat over a much larger area than for a single large-diameter muscle of similar strength.

Textiles and braids that change porosity in response to temperature can potentially be used for clothing that increases wearer comfort or protects emergency responders from intense heat. For instance, movie S7 demonstrates a braid with a coiled nylon muscle inserted in the center. When heated electrically, the muscle contracts, increasing the diameter of the braid, and thereby opening its pores. The braid bias angle and muscle chirality can be selected so that pores either open or close during heating. Using novel textile weaves, comfort-adjusting clothing might be created by combining polymer muscles having large thermal contractions (up to 1.2%/°C, Fig. 4C) with those that thermally expand, to thereby amplify textile porosity changes.

References and Notes

1. Materials and methods are available as supplementary materials on *Science* Online.
2. J. Cui *et al*., *Nat. Mater.* **5**, 286–290 (2006).
3. H. Koerner, G. Price, N. A. Pearce, M. Alexander, R. A. Vaia, *Nat. Mater.* **3**, 115–120 (2004).
4. J. Leng, X. Lan, Y. Liu, S. Du, *Prog. Mater. Sci.* **56**, 1077–1135 (2011).
5. P. Miaudet *et al*., *Science* **318**, 1294–1296 (2007).
6. M. D. Lima *et al*., *Science* **338**, 928–932 (2012).
7. R. H. Baughman, *Synth. Met.* **78**, 339–353 (1996).
8. E. Smela, *Adv. Mater.* **15**, 481–494 (2003).
9. J. L. Tangorra *et al*., *Bioinspir. Biomim.* **2**, S6–S17 (2007).
10. R. Pelrine, R. Kornbluh, Q. Pei, J. Joseph, *Science* **287**, 836–839 (2000).
11. F. Carpi, S. Bauer, D. De Rossi, *Science* **330**, 1759–1761 (2010).
12. Z. Cheng, Q. Zhang, *MRS Bull.* **33**, 183–187 (2008).
13. Y. Kobayashi, A. Keller, *Polymer (Guildf.)* **11**, 114–117 (1970).
14. C. L. Choy, F. C. Chen, K. Young, *J. Polym. Sci. Polym. Phys. Ed.* **19**, 335–352 (1981).
15. L. R. G. Treloar, *Rubber Elasticity* (Oxford Univ. Press, Oxford, 1975).
16. J. Foroughi *et al*., *Science* **334**, 494–497 (2011).
17. F. B. Fuller, *Proc. Natl. Acad. Sci. U.S.A.* **68**, 815–819 (1971).
18. G. H. M. van der Heijden, J. M. T. Thompson, *Nonlinear Dyn.* **21**, 71–99 (2000).
19. J. D. W. Madden *et al*., *IEEE J. Oceanic Eng.* **29**, 706–728 (2004).
20. R. K. Josephson, *Annu. Rev. Physiol.* **55**, 527–546 (1993).
21. J. E. Huber, N. A. Fleck, M. F. Ashby, *Proc. R. Soc. London A* **453**, 2185–2205 (1997).
22. D. Grant, V. Hayward, *IEEE Control Sys.* **17**, 80–88 (1997).
23. Y. Song, X. Chen, V. Dabade, T. W. Shield, R. D. James, *Nature* **502**, 85–88 (2013).
24. M. Zhang *et al*., *Science* **309**, 1215–1219 (2005).
25. Y. Kojima *et al*., *J. Appl. Polym. Sci.* **49**, 1259–1264 (1993).
26. J. M. Hollerbach, I. W. Hunter, J. Ballantyne, in *The Robotics Review* (MIT Press, Cambridge, MA, 1992), vol. 2, pp. 299–342.
27. W. F. Phillips, *Mechanics of Flight* (Wiley, 2004).
28. A. E. Love, in *The Mathematical Theory of Elasticity* (Dover Publications, New York, 1944), pp. 414–417.

Acknowledgments: We thank C. Mozayan, D. B. Hagenasr, Y. Zhang, D. A. Tolly, D. E. Wait, and P. E. Javidnia for assistance with sample preparation and measurements. Support is largely from Air Force Office of Scientific Research grant FA9550-12-1-0211, with additional support from Air Force grants AOARD-10-4067 and AOARD-13-4119, Office of Naval Research MURI grant N00014-08-1-0654, Robert A. Welch Foundation grant AT-0029, the Creative Research Initiative Center for Bio-Artificial Muscle, the Korea–U.S. Air Force Cooperation Program grant 2012-00074 (Korea), Centre of Excellence funding from the Australian Research Council and the Australian National Fabrication Facility, China National 973 Project (nos. 2007CB936203 and S2009061009), NSF China (no. 51003036), and a Natural Sciences and Engineering Research Council of Canada Discovery grant. Correspondence and requests for materials should be addressed to ray.baughman@utdallas.edu. A provisional patent application (61784247) and an international patent application (PCT/US2013/053227) have been filed by N. Li *et al*. on "Coiled and non-coiled twisted nanofiber yarn and polymer fiber torsional and tensile muscles."

Supplementary Materials

www.sciencemag.org/content/343/6173/868/suppl/DC1
Materials and Methods
Supplementary Text
Figs. S1 to S13
Tables S1 and S2
References (*29*–*31*)
Movies S1 to S8

7 October 2013; accepted 23 January 2014
10.1126/science.1246906